ELSEVIER

Polymer 40 (1999) 4615–4627

polymer

The nature of secondary crystallization in poly(ethylene terephthalate)

Z.-G. Wang[a], B.S. Hsiao[a,*], B.B. Sauer[b], W.G. Kampert[b]

[a]*Department of Chemistry, State University of New York at Stony Brook, Stony Brook, NY 11794-3400, USA*
[b]*DuPont Central Research and Development, Experimental Station, Wilmington, DE 19880-0356, USA*

Dedicated to Professor Ronald K. Eby on the occasion of his 70th birthday

Received 28 August 1998; received in revised form 11 November 1998; accepted 19 November 1998

Abstract

The nature of secondary crystallization in poly(ethylene terephthalate) (PET) was examined during isothermal crystallization and subsequent melting by time-resolved synchrotron small-angle X-ray scattering (SAXS), differential scanning calorimetry (DSC) and temperature modulated DSC (MDSC) techniques. In one experiment, the process of isothermal crystallization was sustained over 72 h to induce a relatively large crystallinity (46%, by weight). The purpose of this experiment was to resolve the issue of controversial assignment for the crystal lamellar thickness (l_c) by the correlation function analysis of the SAXS data. Results suggest that a two-stage decrease mechanism exists in both long period (L) and l_c during isothermal crystallization: (1) a significant decrease in the initial stage (primary crystallization dominant), and (2) a much slower decrease in the later stage (secondary crystallization dominant) that is nearly linear with log time. We attribute this behavior to the formation of thinner separate stacks of lamellae between the primary stacks by secondary crystallization. Both secondary and primary stacks can undergo a great deal of crystal perfection and rearrangement with time. From DSC measurements, a triple-melting behavior was observed in the samples crystallized at 205 and 215°C for 1 h, and a double-melting behavior at higher temperatures of 225 and 231°C for 2 h. Temperature scanning SAXS and MDSC directly characterize aspects of crystal perfection and melting. Consistent with some of the literature, we confirm that for short annealing (~ hour) at 200–220°C, the first (low) endotherm is related to melting of secondary crystals, the middle endotherm is due to melting of primary crystals, and the third endotherm is due to melting of crystals reorganized during heating. With prolonged crystallization at 231°C for 24 and 72 h, a single higher melting endotherm was observed even though SAXS experiments indicate a slight decrease in average lamellar thickness. In PET, ester exchange reactions contribute to unusual high mobility, allowing chains to avoid topological constraints such as entanglements and tie chains. The results suggest that the change in population of tie molecules in the non-crystalline phase reduces the entropy of melting causing an increase in T_m, and that this overwhelms the contribution of the decrease in l_c.

Keywords: Poly(ethylene terephthalate); Secondary crystallization; Crystal perfection

1. Introduction

The term ‘‘secondary crystallization’’ is frequently used to describe the effects that will increase crystallinity after the event of primary crystallization. The process of secondary crystallization can usually be identified by the deviation of an Avrami curve at the later stage [1]. However, the nature of the secondary crystallization is still unclear. It could include the thickening of lamellae, perfection of the crystals, or growth of defective crystallites. Recently, we and other laboratories have proposed the mechanisms of lamellar stack insertion and single lamellae insertion as two possible pathways [2] to induce additional crystallites during secondary crystallization of semistiff polymers such as poly(etheretherketone) (PEEK) [2–7] and poly(ethylene terephthalate) (PET) [8–10], based on time-resolved small-angle X-ray scattering (SAXS) results. The lamellar stack insertion mechanism is favored in these polymers and is supported by the data presented here. It was suggested that the mechanism includes effects from crystallization in the ‘‘restrained’’ amorphous regions where the entropy is reduced due to the presence of neighboring stacks [11]. As entropy is decreased, or low molar mass fraction is increased, the formation of crystallites with thinner thickness can become stabilized. It is also known that the high melt viscosity of polymers causes kinetic restrictions. As a result of this, crystal thicknesses rarely reach values even close to their full equilibrium thickness. The low melting secondary crystal development also may be moderated by further kinetic restrictions due to the neighboring

* Corresponding author. Tel.: +1-516-632-7793; fax: +1-516-632-6518.

E-mail address: bhsiao@notes.cc.sunysb.edu (B.S. Hsiao)

0032-3861/99/$ - see front matter
PII: S0032-3861(99)00067-1

crystallites. However, any arguments and models are often undermined by a controversy over the analysis of the SAXS data.

In brief, the controversy stems from the ambivalence of using the correlation function method to determine the crystal thickness from the SAXS data, when the measured polymers have a low degree of crystallinity (usually $< 40\%$) [12,13]. The correlation function method can be used to resolve two quantities, e.g. crystal and amorphous layer thicknesses in lamellar stacks. It, however, cannot determine which value represents which phase. Consequently, in the event that the crystallinity is low, one school of researchers is inclined to assign the smaller value as the crystal thickness because the product of the long period (L, from SAXS) and bulk crystallinity (ϕ_c from WAXD, differential scanning calorimetry (DSC) or density) is often close to the low value [14–19]. Such an assignment suggests that the morphology consists of space-filling lamellar stacks. Other researchers and we however, believe the opposite assignment is correct [2,6–8,10]. As the two thicknesses often exhibit different trends of changes with time during crystallization, the opposing assignments lead to very different interpretations of the morphological development during the crystallization and melting of polymers. For blends with only one semistiff polymer able to crystallize, the interpretation of thermal and morphological properties become even more ambiguous depending on the assignment.

In this study, we intend to revisit the issues relevant to secondary crystallization in PET, and to tackle the problem of the ambivalence in the thickness assignment by the SAXS analysis. The selection of PET is due to the existence of abundant data during secondary crystallization [14–16,20–25], and a well-documented controversy in the SAXS assignment [12,14,15,17,26,27]. In addition, as PET can be viewed as a model system for polymers containing semistiff chains such as polyesters, polyamides and poly(etherketones), we hope results from this study will yield information universal to these polymers. In particular, as secondary crystallization is believed to be important in the multiple-melting behavior in PET [14,16,26,28], this study is intended to improve our understanding of the mechanism of multiple-melting behavior. Currently, very different viewpoints are still present including aspects of melting-recrystallization [17] and dual-populations of lamellar stacks [2,6], which are used separately or in combination to interpret this phenomenon.

2. Experimental

The chosen PET sample is an experimental grade material provided by DuPont Company, which has a number-average molecular weight of 25 000 and a polydispersity (M_w/M_n) of about 2. The glass transition temperature T_g and the nominal melting temperature T_m of this sample are 80 and 270°C, respectively. The samples were vacuum dried for over 24 h prior to X-ray and thermal measurements.

The time-resolved SAXS measurement was carried out using a Braun linear position sensitive detector at the Beamline X3A2 in National Synchrotron Light Source (NSLS), Brookhaven National Laboratory (BNL). The wavelength used was 1.28 Å and the sample to the detector distance was 1345 mm. Isothermal crystallization and subsequent melting of PET was performed by a dual-chamber temperature jump apparatus [3]. The sample was sealed in between two Kapton films with a nitrogen bleed to prevent contact with air. For isothermal crystallization measurement, the experimental procedure was as follows. After being equilibrated at 280°C (10°C above the nominal melting point) for 5 min, the PET sample was rapidly jumped to a second chamber (aligned in the path of the X-ray beam) at temperatures of 205, 215, 225 and 231°C, respectively, for measurements. The total data collection time is 1 h for 205 and 215°C, 2 h for 225 and 231°C, and about 72 h for 231°C. An acquisition time of 10 s per scan was used for 205 and 215°C, 20 s for 225 and 231°C. For the prolonged crystallization measurement at 231°C (72 h), a wait time of 40 s was used between the scans during the first 4 h. After the initial measurement, the experiment was interrupted by another wait period of 68 h. The experiment was resumed again for measurement of 30 min. Subsequent X-ray melting measurements were carried out with a heating rate of 5°C/min after the isothermal crystallization experiment.

Thermal properties of PET samples prepared under similar thermal conditions were also characterized by Perkin–Elmer DSC-7 station and a TA Instruments 2920 DSC for temperature modulated DSC (MDSC) experiments. All samples were annealed and studied under nitrogen environments. In addition to the thermograms taken using similar thermal profiles as in the SAXS measurement, isothermally annealed samples (after dropping from 280°C to the desired melt crystallization temperature) were also scanned at different rates: 5, 10, 20, 30, 40°C/min, respectively, to examine the kinetics dependence of multiple melting transitions.

MDSC is a new technique that subjects a material to a linear heating ramp with a superimposed small amplitude sinusoidal temperature oscillation (modulation) [29]. Deconvolution of the resultant heat flow profile provides not only the ''total'' heat flow obtained from conventional DSC, but also separates that ''total'' heat flow into its heat capacity-related (reversible) and kinetic (non-reversing) components [30]. Exothermic signals are detected only in the non-reversible data, but endothermic melting behavior can contribute to both reversible and non-reversible signals [30]. For all experiments a heating ramp of 2°C/min was chosen and a modulation frequency and amplitude of 0.32 min^{-1} and 1°C were used, respectively, based upon the recommended specifications of the instrument supplier (Thermal Analysis DSC2920), and our experience with PET. This selection of amplitude and frequency for the

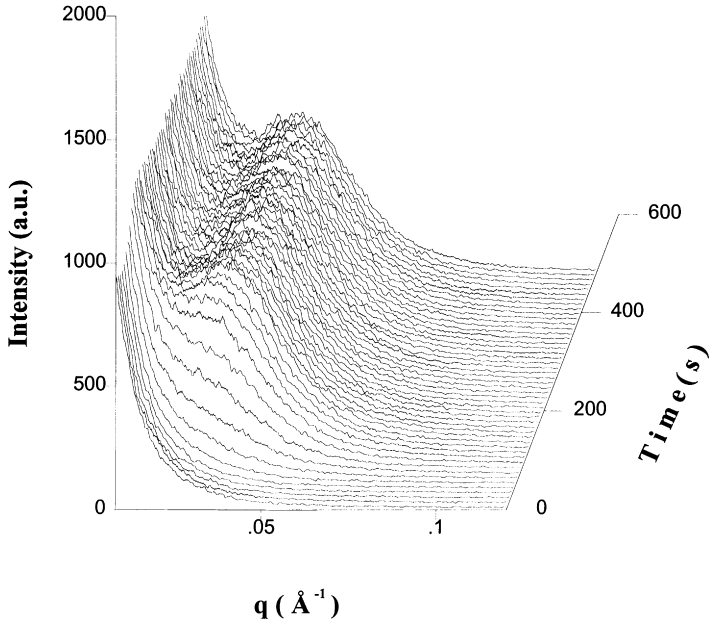

Fig. 1. Time-resolved SAXS profiles as collected during isothermal crystallization process of PET at 205°C.

sinusoidal modulation contributes to high sensitivity and resolution.

3. Results

3.1. SAXS study during isothermal crystallization

The procedures for calculating the morphological parameters from the time-resolved SAXS data of semicrystalline polymers have been discussed earlier by us [31]. They involve the use of correlation function to extract morphological parameters such as scattering invariant (Q), long spacing (L), lamellar thickness ($l_1 = l_c$) and amorphous interlayer thickness ($l_2 = l_a$).

Typical real-time SAXS profiles and Lorentz corrected scattering profiles at 205°C are shown in Figs. 1 and 2, respectively. During the induction period (ca. 80 s), one observes only diffuse scattering curves without scattering maxima. Above 80 s, a distinct scattering maximum appears, which progressively moves to a higher scattering angle with time. These changes are accompanied by an increase in the intensity. Fig. 3 shows one-dimensional correlation function profiles obtained from the data in

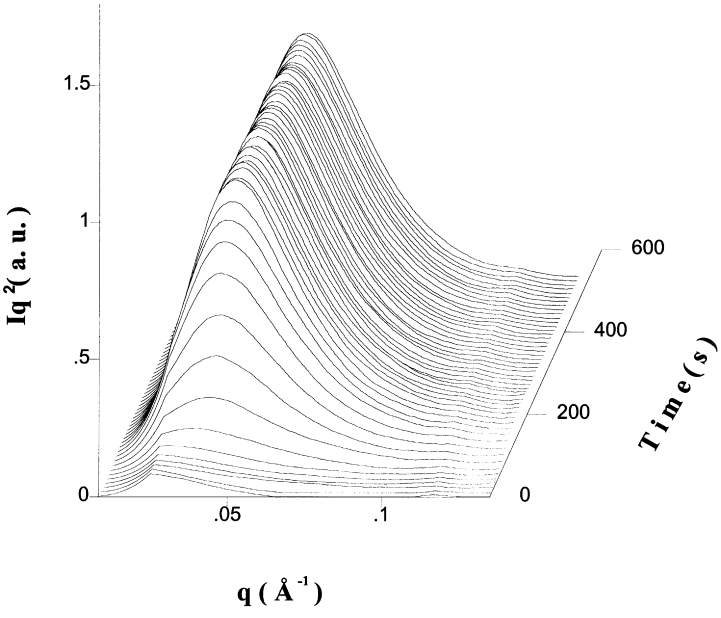

Fig. 2. Lorentz corrected SAXS profiles from Fig. 1; the data was corrected for background, liquid-like scattering and the interface.

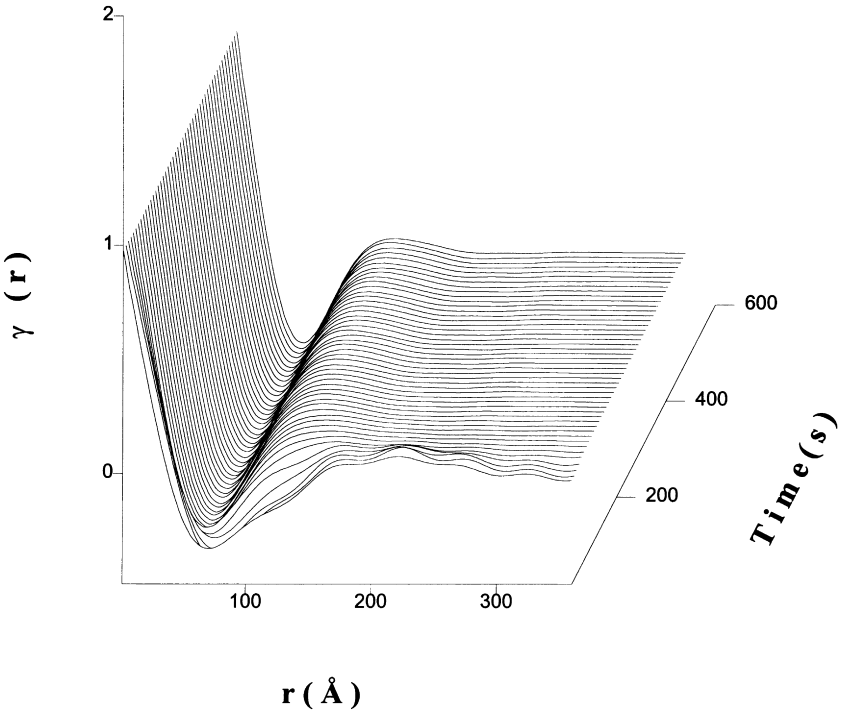

Fig. 3. Corresponding one-dimensional correlation function profiles obtained from the data in Fig. 2.

Figs. 1 and 2. The long period L can be obtained from the first maximum of the correlation function, which is found to be a function of temperature and time (as shown in Fig. 4). It is seen that the value of L decreases with crystallization time. Fig. 5 illustrates corresponding changes in the value of Q as a function of time at different temperatures. A characteristic time t_c, at which half of the change in Q occurs, can be defined in Fig. 5. Fig. 6 illustrates the effect of crystallization temperature on t_c, which resembles the conventional crystallization half-time plot from DSC. We have also obtained the morphological parameters l_1 and l_2 (thicknesses of the two constituent scattering phases) from the analysis of correlation function. We have assigned the larger value as the lamellar thickness, l_c, and the smaller value as the amorphous layer thickness, l_a. The reason for this assignment is the centerpiece of this article and will be discussed in detail later in the discussion section (Section 5). The changes in l_c and l_a with time as a function of crystallization temperature are shown in Figs. 7 and 8, respectively. It is seen that the decrease in l_c are quite significant with time at all temperatures, while the decrease in l_a are smaller. Two interesting observations can be made in Figs. 4, 5, 7 and 8. First, during the primary crystallization dominant stage, both L, and l_c exhibit a significant decrease. In this stage, Q exhibits a sigmoidal increase with time. Second, during the secondary crystallization stage, both L, and l_c exhibit a lesser decay that is approximately linear with log time. In the second stage, Q appears to increase very slightly with time.

To explore more details in the secondary crystallization

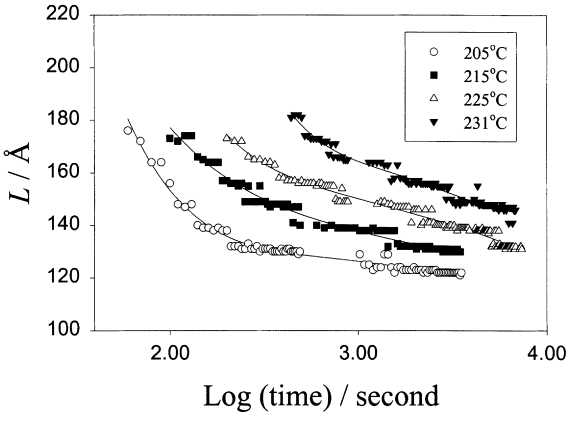

Fig. 4. Time evolution of long period, L, during isothermal crystallization at 205, 215, 225 and 231°C, respectively.

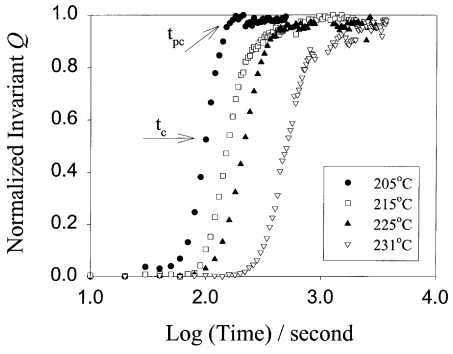

Fig. 5. The changes of the invariant, Q, during isothermal crystallization at 205, 215, 225 and 231°C, respectively.

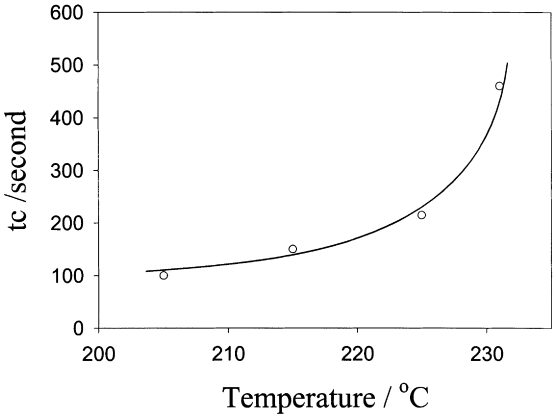

Fig. 6. Half time t_c, determined from the change of Q in Fig. 5 as a function of crystallization temperature.

stage, we have collected the synchrotron SAXS data at 231°C for over 72 h. The prolonged annealing has enabled the sample to complete the secondary crystallization process, with a small increase in molecular weight due to solid state polymerization. The corresponding changes of long period, lamellar thickness and amorphous layer thickness with time are shown in Fig. 9. As the induced crystallinity is high in this measurement (bulk crystallinity of 46% by weight or 43% by volume, as measured by DSC), we can positively assign the higher value of the thickness as the thickness for crystalline lamellae and the low value as the thickness for amorphous layer. The detailed justification will be given later. Similar to the observations made earlier in lower temperature and shorter time measurements [2], we found that both L and l_c decrease significantly during the initial primary crystallization stage and decay linearly at a slower rate in the secondary crystallization stage (L and l_c are 133 and 84 Å after 2 h, and 116 and 69 Å after 72 h). In contrast to the large changes in L and l_c, the variation of l_a is much smaller.

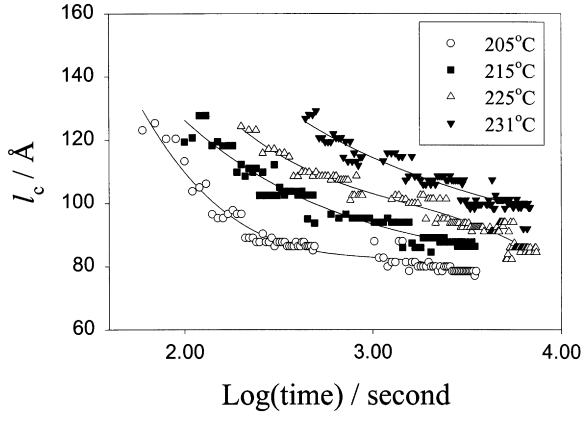

Fig. 7. The variation of lamellar thickness, l_c, with time at 205, 215, 225 and 231°C, respectively.

3.2. DSC characterization of isothermal crystallized samples

DSC measurements were used to characterize the thermal and reorganization behavior of the annealed PET samples. Heating scans of samples isothermally crystallized at 205°C for 1 h at different rates (5, 10, 20, 30 and 40°C/min) are shown in Fig. 10. For this crystallization temperature, a ''triple-melting'' behavior is seen, which is persistent at all heating rates used here. These results are consistent with some earlier reports [32,33] that the first and second endotherms increase in size as the heating rate increases. The first endotherm is associated with the subsidiary (secondary) crystal melting, and the second endotherm is related to the melting of primary stacks formed during annealing at T_c, and the last endotherm is due to melting of crystals perfected during the heating scan.

MDSC is a new tool [29] that provides important information confirming that the third endotherm in this sample is due to reorganized crystals formed during the heating scan (Fig. 11), and that the lowest endotherm is associated with the onset of a substantial degree of melting and recrystallization. Examination of the reversible and non-reversible scans in Fig. 11 shows a strong pre-melting (endotherm) and recrystallization (exotherm), respectively, starting at about 215°C. The recrystallization is strong evidence that recrystallization and perfection is a rapidly nucleated process. Rapid nucleation is attributed to the presence of existing nuclei due to partial melting which leaves substantial levels of nuclei behind. As a result of the high crystallization temperature, these are naturally characterized by a high T_m of about 258°C, contributing to the third endotherm.

We can also draw other conclusions from the MDSC data in Fig. 11. The low endotherm region is seen to consist of complicated contributions from simultaneous offsetting exothermic and endothermic processes, with exothermic signals only detected in the non-reversible signal, and endothermic contributions detected in both reversible and non-reversible signals as is known in the literature [29]. It is clear that with the total DSC scan alone, one cannot obtain the complete information.

The variable heating rate DSC data give an indication that the third endotherm is due to recrystallization, and MDSC gives quantitative details of the recrystallization but require some skill and background in interpretation. Therefore, we now present macroscopic evidence obtained by rapidly heating a thin (0.5 mm) film of a 200°C (2 h) annealed PET by quickly pressing against a temperature controlled metal surface at 245°C. We have proved that it completely melts even though it is below the third endotherm temperature (third endotherm at ~ 257°C), by observing the viscosity of the liquid, or by quenching and characterizing by DSC which shows that the sample is completely amorphous. Zachmann and Stuart have performed similar experiments and reached

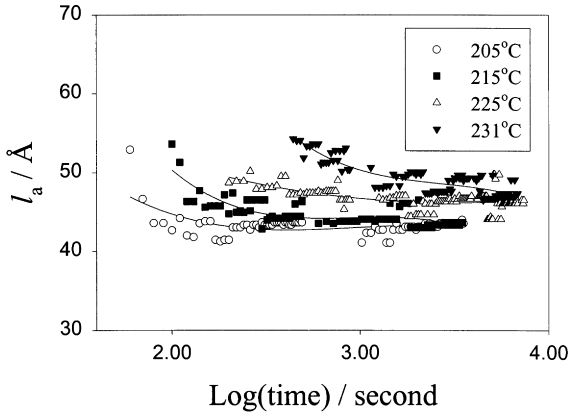

Fig. 8. The variation of amorphous layer thickness, l_a, with time at 205, 215, 225 and 231°C, respectively.

the same conclusion [34]. Thus, the third 258°C endotherm is directly proven to be due to sample perfection caused by DSC heating.

Figs. 12 and 13 show the corresponding DSC results at crystallization temperatures of 215°C for 1 h and 225°C for 2 h, respectively. The triple-melting behavior is still apparent for 215°C but only a double-melting behavior is seen for 225°C. To summarize, in 205 and 215°C scans, there is a small endotherm between 225–235°C, a middle endotherm between 240 and 250°C and a final endotherm at around 255°C. In 225°C scans, the first small endotherm moves into the middle endotherm, giving rise to a double-melting behavior, which has been broadly reported previously [15,18,32]. These endotherm intensities are slightly different from those previously reported [26], where the first endotherm does not disappear with increased temperature. However, the behavior of the second endotherm is consistent with that report, which increases its size and shifts to a higher value with heating rate with the expense of the third endotherm. This difference is probably because of different variables in crystallization time, temperature and molecular

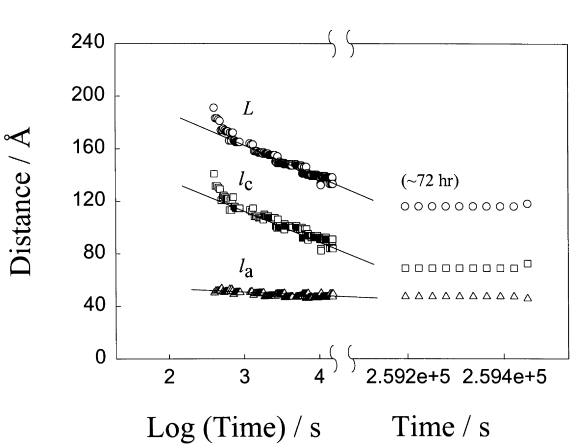

Fig. 9. The change of L, l_c, and l_a for PET during prolonged isothermal crystallization at 231°C for 72 h.

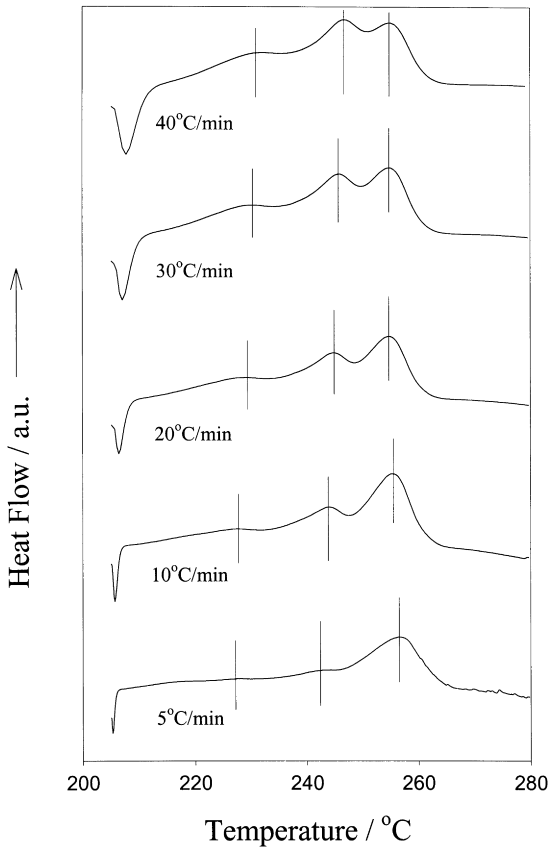

Fig. 10. DSC traces of PET after isothermal melt crystallization at 205°C for 1 h as a function of heating rate.

weight [26]. In all cases the DSC scan is modifying the sample, and we emphasize that the highest peak is due to perfection of crystals during the heating scan.

With increasing heating rate, the melting positions of the first and second peaks move significantly toward higher values, but the position of the third peak is relatively constant. Such a multiple-melting behavior in PET has been reported several times and the number of melting

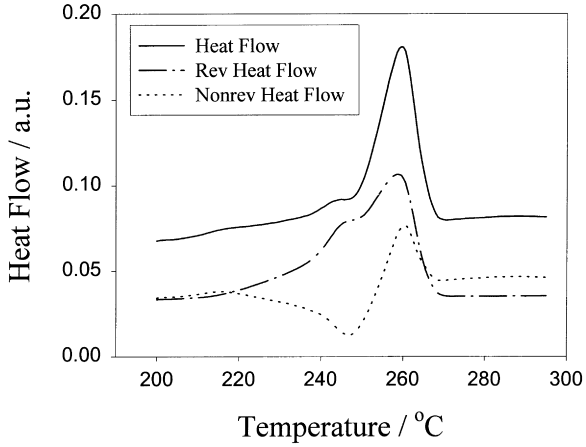

Fig. 11. Modulated DSC data for PET melt crystallized by annealing at 205°C for 1 h.

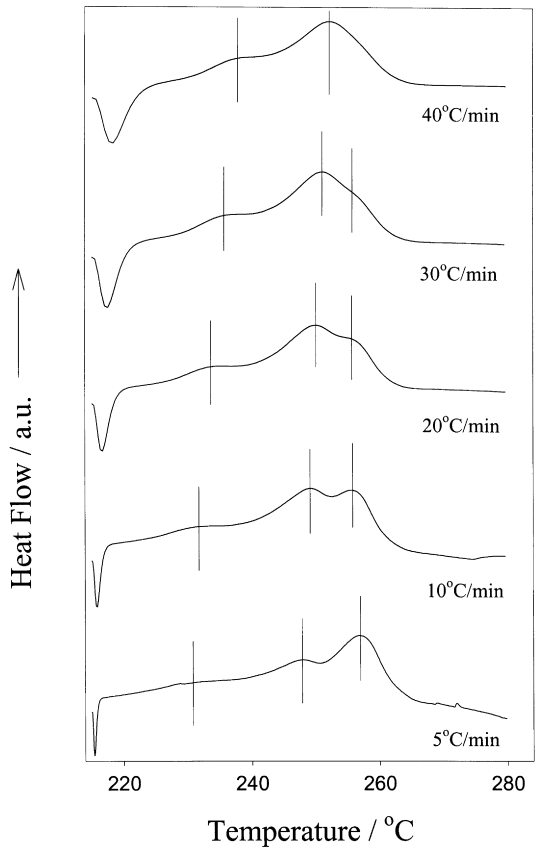

Fig. 12. DSC traces of PET after isothermal melt crystallization at 215°C for 1 h as a function of heating rate.

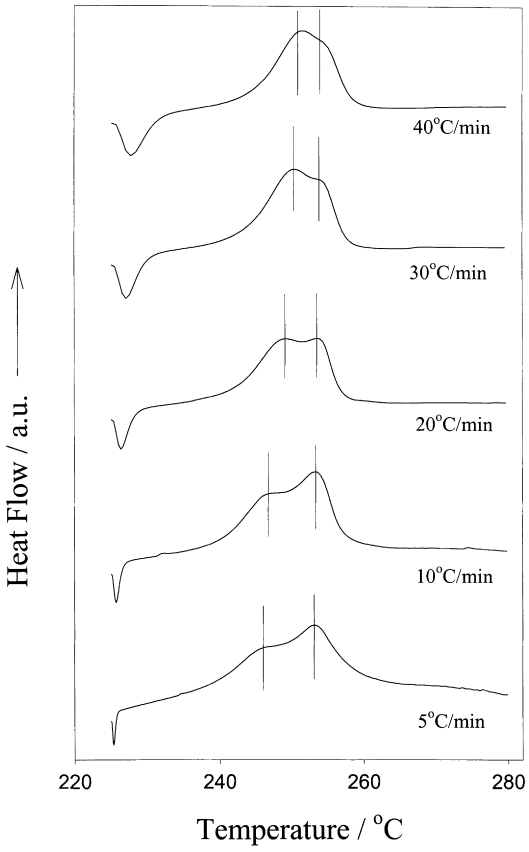

Fig. 13. DSC traces of PET after isothermal melt crystallization at 225°C for 2 h as a function of heating rate.

endotherms, ranging from one to three or more, depends on the thermal history [14–16,23,25,26,28,35]. Several different models were used to explain the PET multiple-melting processes. These models will be evaluated with our results in Section 3.3.

With prolonged crystallization at 231°C, very different results are seen (as shown in Fig. 14). It can be found that the double-melting endotherms are present for crystallization of 2 h, but a single-melting endotherm appears after 24 and 72 h. The position of the endotherm moves to a higher temperature with longer annealing time. This indicates that the structure of the crystal perhaps is improved by modification of both primary and secondary crystallites, which become almost equivalent. Such modification is accelerated by chemical reactions outside of the crystals and will not be the same for all polymers. MDSC data for the samples annealed at 231°C for 2 and 72 h are given in Figs. 15 and 16, respectively. In Fig. 15, the data show the endotherm consisting of almost equal fractions of reversible and non-reversible contributions. In Fig. 16, the data show a narrow endotherm at 264°C. In Figs. 15 and 16, there are no well separated exotherms indicating recrystallization, although we suspect that some reorganization in the 2 h sample contributes to some of the signal in the high endotherm region in Fig. 15.

3.3. SAXS studies of subsequent melting process

Next we will investigate morphological changes during subsequent melting of samples after isothermal crystallization at different temperatures by SAXS. Results obtained from the correlation function analysis are shown in Figs. 17–19, which illustrate the changes in L, l_c, and l_a with

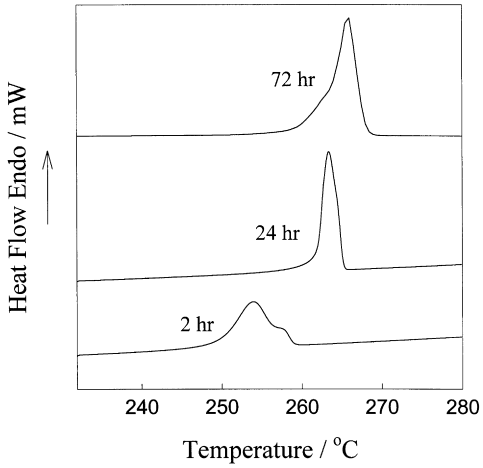

Fig. 14. DSC traces of PET after isothermal melt crystallization at 231°C for 2, 24 and 72 h, respectively.

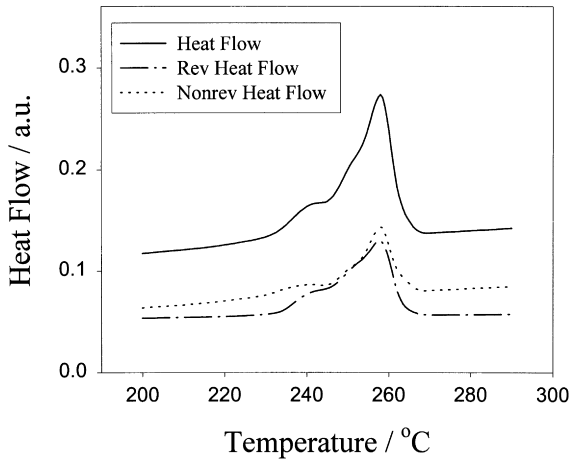

Fig. 15. Modulated DSC thermograms from sample annealed at 231°C for 2 h.

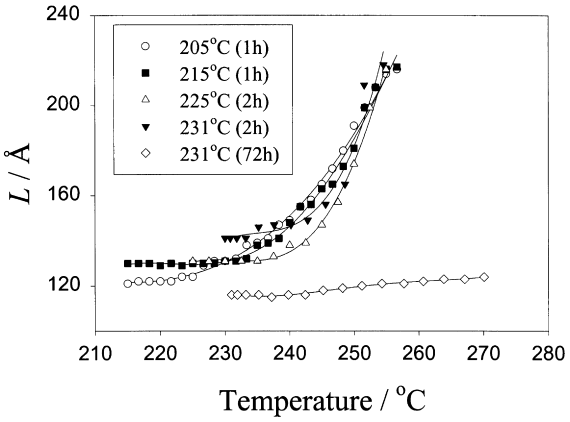

Fig. 17. The changes of L during subsequent heating process after isothermal melt crystallization at different temperatures.

temperature. For isothermal crystallization at a relative short time (1–2 h), the values of L and l_c are found to increase rapidly once melting begins. In contrast, after prolonged crystallization at 231°C, L and l_c show only a slight increase at temperatures even near complete melting. In Figs. 17–19, the temperature of isothermal crystallization has a negligible effect on L, l_c, and l_a except for 231°C.

Comparisons between synchrotron SAXS and DSC results are made during subsequent melting to reveal the mechanism of multiple melting behavior (Figs. 20–23). Both measurements were carried out with identical thermal histories and the chosen heating rate was 5°C/min. In the case of triple-melting behavior (Fig. 20, isothermal crystallization at 205°C for 1 h), L is found to rise immediately after the first endotherm, while Q remains about constant. Near the second endotherm, L continues to increase but with no step-change appearance, while Q begins to decrease sharply. The large degree of melting and reorganization detected by MDSC for this sample starting at about 220°C (Fig. 11), is consistent with the large increase in L (or large increase in l_c), and sharper decrease in Q in the region of the third endotherm.

At the peak temperature of the final endotherm, L can no longer be determined as there is no identifiable scattering maximum, while Q continues to decrease in accord with the DSC heat flow trace. For the triple-melting behavior induced at a different temperature (Fig. 21, 215°C for 1 h), very similar trends of changes in Q and L are seen. By using higher isothermal crystallization temperatures at 225 and 231°C (Figs. 22 and 23), a nominal double-melting behavior is obtained. In these measurements, the changes in Q and L are similar to those in the triple-melting curve, except the melting temperatures are shifted. The detectable final value of L is found to be near the transition temperature of the highest endotherm. The corresponding value of Q at this temperature appears to be near the inflection point of the total decrease in Q.

Also included in Fig. 23 are melting results from the prolonged annealed sample at 231°C for 72 h. It is interesting to note that a single DSC endotherm (although with a broad low temperature tail) is present at a higher temperature and the value of L only increases slightly

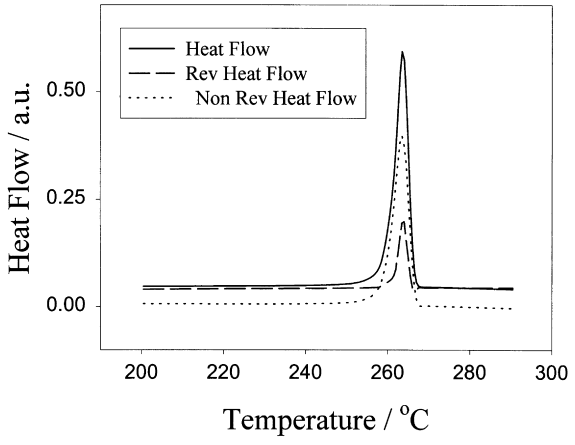

Fig. 16. Modulated DSC thermograms from sample annealed at 231°C for 72 h.

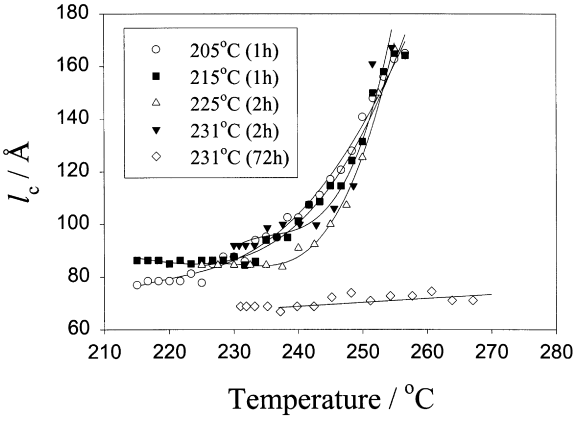

Fig. 18. The changes of l_c during subsequent heating process after isothermal melt crystallization at different temperatures.

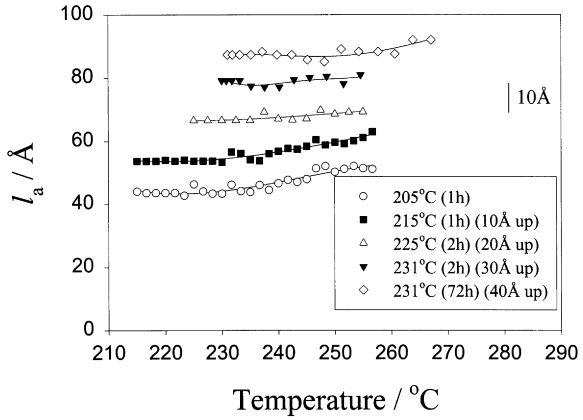

Fig. 19. The changes of l_a during subsequent heating process after isothermal melt crystallization at different temperatures.

with temperature even when the sample is almost completely melted. However, the changes in Q are similar to those before but occur at a higher temperature.

4. Discussion

The ambivalence of lamellar thickness determination from the correlation function or related methods has slowed our understanding of the crystallization process. The correlation function method only yields the thickness values for the constituting phases (l_1 and l_2) rather than defining the crystal lamellar thickness or amorphous layer thickness (l_c and l_a). As mentioned previously, we have assigned the larger value l_1 as l_c and smaller value l_2 as l_a. Our reasons are as follows. For PET sample crystallized at 231°C for 72 h, the final bulk crystallinity in mass ϕ_c is about 46% (determined from DSC, $\Delta H = 63$ J/g, and for 100% crystalline PET $\Delta H = 138$ J/g [1]). The bulk crystallinity in volume $X_c(= \phi_c(\rho/\rho_c))$ thus is about 43%. The high temperature WAXD measurement has also confirmed this value. Time-resolved morphological results from the correlation function analysis are shown in Fig. 24. In this figure, it is seen as before that both L and l_1 decrease significantly at the early stage and then decay at a much slower rate (almost linear) with log time. The corresponding value of l_2 remains about constant. After prolonged annealing for 72 h, the final value of L is 116 Å, l_1 is 69 Å and l_2 is 47 Å, which suggests that the linear crystallinity (within the lamellar stacks) is either ($\chi_L = l_1/L$) 59.5% or ($\chi_L = l_2/L$) 40.5%. The assignment of $\chi_L = 40.5\%$ does not make sense, as it cannot be lower than the bulk crystallinity in volume of 43% (otherwise, the volume fraction of lamellar stacks in bulk sample becomes larger than 1). The difference of 2.5% (43 versus 40.5%) is small but significant, as we know that both DSC and WAXD methods underestimate the true value of volume crystallinity due to crystal defects and thermal effects (WAXD). The assignment of l_1 as the lamellar thickness thus suggests that the value of volume fraction of lamellar stacks is only 72% even after 72 h. This implies that the crystallization of PET stacks does not result in the complete space-filled morphology. This may be reasonable when one considers the fractions of non-crystallizable species (impurity, chain branches…) that may aggregate into irregular domains after prolonged annealing and the other kinetic constraints because of the high molecular weight.

It was found that, during the isothermal crystallization process at long times, both L and l_c decrease significantly, especially after primary crystallization is complete. These decreases can be explained by the formation of two populations of lamellar thickness at the different stages of crystallization. We define the earlier stage ($t < t_{pc}$, where t_{pc} is the onset time of the plateau Q value in Fig. 5) as the primary crystallization dominant stage. In this stage, both L and l_c exhibit a significant decrease and Q exhibits a sigmoidal rise. We attribute the initial steeper decreases to the growth of thinner stacks of lamellae between the existing thicker primary lamellar stacks (the stack insertion model). These thinner stacks are very similar to primary stacks, and form quite rapidly probably as branches within the spherulite. In a way, their formation is simply a way for the system to fill the space as completely as possible. We do not favor the

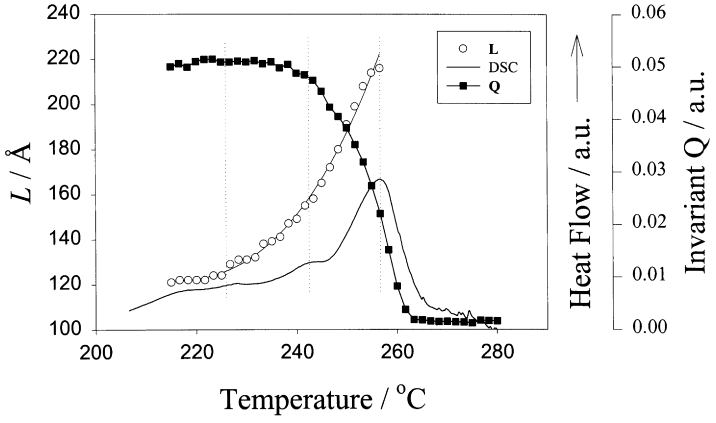

Fig. 20. The comparison of changes in L, Q, and DSC trace during subsequent heating after isothermal crystallization at 205°C for 1 h.

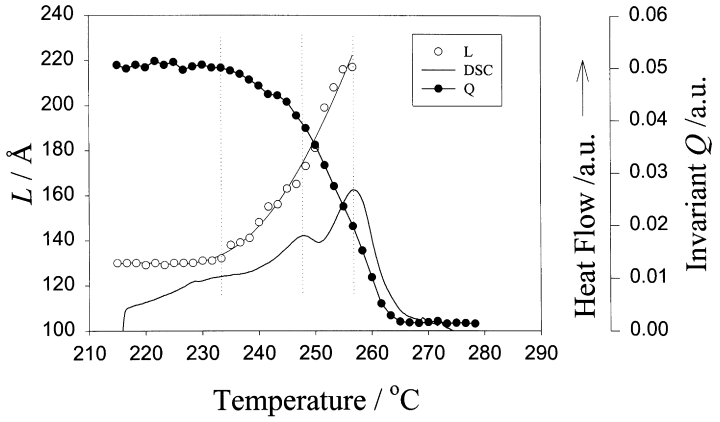

Fig. 21. The comparison of changes in *L*, *Q*, and DSC trace during subsequent heating after isothermal crystallization at 215°C for 1 h.

lamellar insertion model (secondary lamellae occur within the primary stacks) as the change in l_a is relatively small during crystallization (also upon subsequent melting). Also, l_a is much too small and the species far too topologically constrained to allow lamellae formation within an existing stack.

At the later stage, *L* and l_c exhibit slower decays that are approximately linear with log time. We attribute this stage to the secondary crystallization dominant stage, where the event of primary crystallization is absent. The slower decreases in *L* and l_c indicate that the formed crystallites are thinner and more defective. It is also consistent with the small but visible changes in crystallinity by DSC and WAXD after annealing of intermediate time (for example, as seen by black circles in Fig. 24), which is also found to be linear with log time. With prolonged annealing at high temperatures (231°C, 24 or 72 h), the morphological parameters in PET may be influenced by transesterification which will be discussed in more detailed later.

The formation of two populations of lamellar thickness during an isothermal process can be understood from a kinetic and thermodynamic viewpoint, and these are difficult to separate at this time. As crystallization first takes place in the ''virgin'' melt producing lamellar stacks with thickness that is mainly a function of the degree of supercooling, we term this process as primary crystallization. In the event that the primary stacks or fibrils are formed but not in a space-filling fashion, subsequent crystallization can take place in the ''restrained'' amorphous regions imposed by the primary lamellar stacks (also molecular impurities and low molar mass fractions). For the thermodynamic model, we term the process of subsequent crystallization from these ''restrained'' amorphous regions (with reduced entropy that increases the effective melting point) as secondary crystallization. The process of secondary crystallization is obviously heterogeneous and depends not only on the presence of primary crystallites, but also the formation of earlier formed secondary crystallites. In principle, the process of secondary crystallization can occur continuously until the available amorphous regions are totally consumed. We thus believe that isothermal crystallization should always produce two populations of lamellar thickness in polymers: (1) the thicker lamellae formed first at the primary crystallization stage and (2) the thinner lamellae (of a greater heterogeneous distribution),[1] both during and after primary crystallization. However, not all the effects from secondary crystallization can be observed. This is because the different polymers may have different abilities to heal or perfect the crystal defects in secondary crystallites, which also depends on the chain mobility in the crystallizing environment.

Triple-melting endotherms in PET have been reported by Zhou and Clough before [32], who have used a combination of dual lamellar population model and melting-recrystallization model to explain this behavior. The three melting endotherms were labeled as I, II, and III, respectively, in the order of melting point. The first melting endotherm (I) was assigned as the melting of the subsidiary lamellae (from secondary crystallization) and the second endotherm (II) was assigned as the melting of the dominant lamellae, and most literature verifies that the highest endotherm is due to recrystallization [15,18,25,28,32,34]. The third melting endotherm (III) was attributed to the melting and recrystallization process. This explanation is different from a recent report by Medellin-Rodriguez et al. [16,26]. It was proposed that the first endotherm (I) was associated with the final stage of secondary crystallization (small branches of metastable crystalline material), the second endotherm (II) was associated with the secondary crystallization (mainly metastable secondary branches), and the third endotherm (III) was due to the primary crystals undergone some degrees of recrystallization during heating scan. Our data do not support this viewpoint for reasons to be described below.

We now turn our attention to the evaluation of different morphological models to explain the multiple-melting behavior by using SAXS and MDSC results. The

[1] As $T_m = \Delta H/\Delta S$, T_m increases as ΔS decreases. This suggests that, in the restrained melt, the thin lamellae can be stabilized (with the increase in T_m) by the reduced entropy.

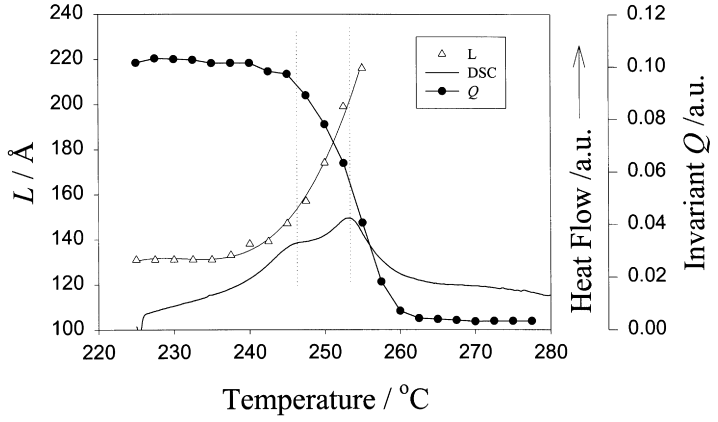

Fig. 22. The comparison of changes in *L*, *Q*, and DSC trace during subsequent heating after isothermal crystallization at 225°C for 2 h.

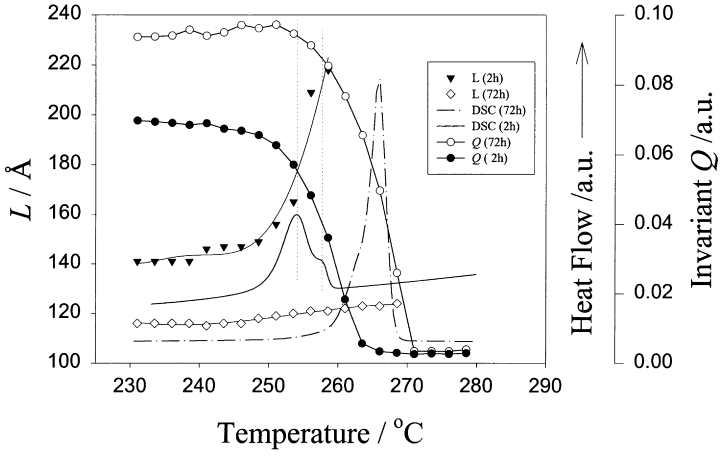

Fig. 23. The comparison of changes in *L*, *Q*, and DSC trace during subsequent heating after isothermal crystallization at 231°C for 2 and 72 h, respectively.

annealing-induced multiple-melting behavior has been observed in many polymers, which is now considered a universal behavior in polymers with semistiff chain [2]. Various models have been proposed to explain this behavior. The two primary models are: (1) melting and recrystallization model and (2) dual population of lamellar thickness model. The view of the melting and recrystallization model has been used to explain the double-melting behavior in PET before [15,23–25,28,34,35]. Based on this model, as the initial lamellae melt and give rise to the

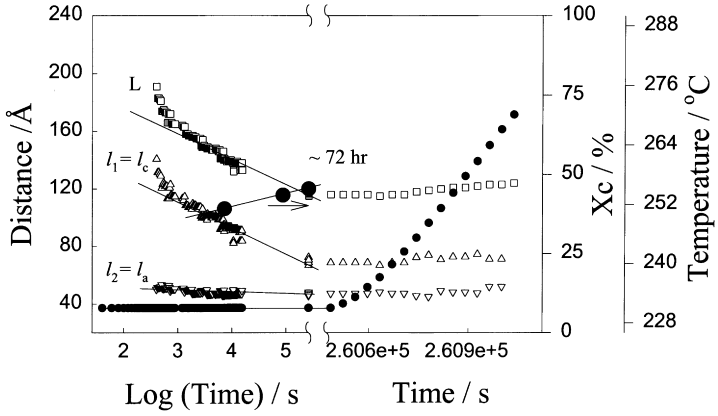

Fig. 24. Time evolution of morphological parameters, *L*, l_c and l_a from SAXS and the degree of crystallinity from DSC during isothermal crystallization at 231°C for 72 h.

low endotherm, the molten material can undergo a recrystallization process during the DSC scan and form thicker lamellae. The recrystallized lamellae melt at a higher temperature and result in the high endotherm. Our results indicate that the multiple-endotherms are probably due to a hybrid of these two mechanisms, and MDSC is a very powerful new tool to quantify the onset temperature and extent over which recrystallization occurs (Fig. 11). Note that in Fig. 11 the onset of pre-melting at about 210°C is detected in total and reversible signals, but exothermic events also begin at about the same temperature. The exothermic recrystallization peaking at about 245°C is very convincing as to the large level of recrystallization, and is a new dimension in our understanding which must be applied to systems in the future. In Figs. 22 and 23, the double-melting endotherms are shown to accompany the changes of L, l_c and Q. The continuous rise in L and l_c is consistent with the dual population lamellar thickness model, but MDSC (Fig. 11) shows the onset of a large crystallization exotherm at about the temperature which L first begins to increase (compare Figs. 11 and 20). This is a direct proof that crystal reorganization is causing much of the increase in L in Fig. 20 for melting of the 1 h, 205°C annealed sample. MDSC shows that the highest endotherm is associated with the recrystallized (reorganized) primary and secondary lamellae, e.g. the recrystallization exotherm in Fig. 11. The second endotherm in triple-melting (Fig. 10 and total heat flow in Fig. 11) thus can be explained by the melting of the primary virgin lamellae. Again the value of MDSC is that it shows that this second endotherm is deceivingly small in total DSC because it is offset by the strong exothermic recrystallization process occurring simultaneously (Fig. 11). The first endotherm in triple-melting evolves over a long time scale and also shifts to higher temperatures with long times over the time period which the SAXS lamellar thicknesses decrease slowly. These factors indicate that this endotherm is due to secondary crystals. At very long times these eventually become similar to primary crystals. The appearance of this low endotherm is pronounced at lower crystallization temperatures when the chain mobility during crystallization is low, but it merges into the middle endotherm at higher crystallization temperature when the mobility is high.

With multiple-endotherms, the heat of fusion of the lower endotherm due to the secondary lamellae was found to increase with annealing temperature and time, which suggests that the defective structure in secondary crystallites can improve. In the extreme case of the prolonged annealing at 231°C for 24 and 72 h (in nitrogen), the lower endotherm is found to be completely eliminated resulting in a single-endotherm melting behavior. The increase in the melting temperature (T_m = 253, 263 and 266°C for 2, 24 and 72 h, respectively) is an indication of morphology changes. At prolonged annealing time, both values of L and l_c were found to be smaller, and one would normally expect lamellar thinning to lead to a lower T_m instead of a higher one. This trend of smaller L and larger T_m was also seen by Zachmann and Schmidt before [25,36]. We attribute the increase in T_m and decrease in l_c (for crystallization at 231°C for 72 h) to transesterification accelerating a change of conformation in the amorphous phase as main-chain bonds are broken outside of the crystal. The explanation has been given earlier by Wunderlich,[2] where he shows that the formation of a higher population of tie molecules and loose loops at the expense of folded chains in PET. These changes in the non-crystalline phase evidently lead to a higher T_m because of a smaller entropy change (ΔS_m) during melting, i.e. $T_m = \Delta H_m/\Delta S_m$, where ΔH_m is the enthalpy of melting.[2] Superheating also results from these changes, and is observed for a variety of high temperature crystallized PET systems.[2] Finally, as the average lamellar thickness decreases, a small perfection also takes place in the lateral directions of the lamellae.[3]

5. Conclusions

The evolution of morphological changes during isothermal crystallization and subsequent melting was followed by synchrotron SAXS and DSC measurements to explore the nature of secondary crystallization in PET. From the large crystallinity (46% in weight and 43% in volume) generated by prolonged annealing, we have proved that the crystal lamellar thickness is the larger value obtained from the correlation function analysis of the SAXS data. The variations of long period, lamellar thickness, amorphous interlayer thickness and the invariant during isothermal crystallization are in favor of the dual population lamellar stacks model. Results indicate two stages in the decrease in long period and lamellar thickness.

These decreases are due to a complicated process of secondary crystallization, which produces thinner lamellar thickness causing the average value to drop. The multiple-melting behavior induced at different temperatures is due to a combination of the dual lamellar stacks model and the melting-recrystallization model. The highest endotherm is associated with the recrystallization process (as indicated by the effect of scanning rate and even more quantitatively in the MDSC results). For PET annealed at high temperatures for up to 72 h, the steady decrease of l_c and simultaneous increase in T_m seem to contradict each other. We base our interpretation on Wunderlich's data, which suggests that the

[2] Ref. [1], page 427.

[3] We have carried out powder X-ray diffraction measurements of the samples crystallized at 231°C for 2 and 24 h, which exhibited an approximately 10% increase in the lateral size for the latter obtained by the line-broadening analysis of the (010) reflection at a d-spacing of 5.03 Å. In addition, we found that the heating-induced reorganization process is significantly retarded by prolonged annealing. This is seen in modulated DSC scans of the sample crystallized at 231°C for 72 h (Fig. 16), where the data show that no significant recrystallization can take place upon heating.

increased melting point arises from a change in conformation of the non-crystalline chains between lamellae causing a lowered entropy of melting.

Acknowledgements

We thank Dr K. Gardner and Ms J. Freida for their work on the wide-angle X-ray diffraction. The authors acknowledge the financial support of this work by a grant from NSF (DMR 9732653) and a DuPont Young Faculty grant. The authors would also like to thank Dr F. Yeh, Mr Z. Cheng and Mr H. Yang for their assistance of the synchrotron SAXS measurement.

References

[1] Wunderlich B. Macromolecular physics, vol. 2. New York: Academic Press, 1976.
[2] Verma RK, Hsiao BS. Trends in Polym Sci 1996;4:9.
[3] Bassett DC, Olley RH, Raheil IAM. Polymer 1988;29:1745.
[4] Hsiao BS, Gardner KH, Wu DQ, Chu B. Polymer 1993;34(19):3986.
[5] Lattimer MP, Hobbs JK, Hill MJ, Barham PJ. Polymer 1992;33:3971.
[6] Verma R, Marand H, Hsiao B. Macromolecules 1996;29:7767.
[7] Verma RK, Kander RG, Velikov V, Marand H, Chu B, Hsiao BS. Polymer 1996;37(24):5357.
[8] Wang ZG, Hsiao BS, Sauer BB, Kampert WG. ACS PMSE Preprint 1998;79;320.
[9] Elsner G, Koch MHJ, Bordas J, Zachmann HG. Makromol Chem 1981;182:1263.
[10] Santa-Cruz C, Stribeck N, Zachmann HG, Balta-Calleja FJ. Macromolecules 1991;24:5980.
[11] Hsiao BS, Sauer BB, Verma R, Chu B, Harney P, Zachmann HG, Seifert S. Macromolecules 1995;28:6931.
[12] Strobl GR, Schneider M. J Polym Sci Polym Phys Ed 1980;18:1343.
[13] Vonk CG, Kortleve G. Colloid Polym Sci 1967;220:19.
[14] Medellin-Rodriguez FJ, Phillips PJ, Lin JS. Macromolecules 1996;29:7491.
[15] Groeninckx G, Reynaers H, Berghmans H, Smets G. J Polym Sci Polym Phys 1980;18:1311.
[16] Medellin-Rodriguez FJ, Phillips PJ, Lin JS, Avila-Orta CA. J Polym Sci Polym Phys 1998;36:763.
[17] Jonas AM, Russell TP, Yoon DY. Colloid Polym Sci 1994;272:1344.
[18] Lee Y, Porter RS. Macromolecules 1987;20:1336.
[19] Lee Y, Porter RS, Lin JS. Macromolecules 1989;22:1756.
[20] Schultz JM, Fakirov S. Solid state behavior of linear polyesters and polyamides. New Jersey: Prentice Hall, 1990.
[21] Imai M, Kaji K, Kanaya T, Sakai Y. Phys. Rev. B 1995;52(17):12696.
[22] Stribeck N. Colloid Polym Sci 1993;271:1007.
[23] Alfonso GC, Pedemonte E, Ponzetti L. Polymer 1979;20:104.
[24] Sweet GE, Bell JP. J Polym Sci A-2 1972;10:1273.
[25] Holdsworth PJ, Turner-Jones A. Polymer 1971;12:195.
[26] Medellin-Rodriguez FJ, Phillips PJ, Lin JS, Campus R. J Polym Sci Polym Sci 1997;35:1757.
[27] Goschel U, Urban G. Polymer 1995;36:3633.
[28] Fontaine F, Ledent J, Groeninckx G, Reynaers H. Polymer 1982;23:185.
[29] Reading M, Elliot D, Hill VL. J Thermal Anal 1993;40:949.
[30] Okazaki I, Wunderlich B. J Polym Sci Polym Phys 1996;34:2941.
[31] Hsiao B, Verma R. J Synchrotron Rad 1997;5:23.
[32] Zhou C, Clough SB. Polym Engng Sci 1988;28:65.
[33] Medellin-Rodriguez FJ, Phillips PJ. Macromolecules 1995;28:7744.
[34] Zachmann HG, Stuart HA. Makromol Chem 1960;41:148.
[35] Roberts RC. Polym Lond 1969;10:117.
[36] Zachmann HG, Schmidt GF. Makromol Chem 1962;52:23.